Available online at www.sciencedirect.com
ScienceDirect
Journal of the European Ceramic Society 28 (2008) 1443–1449
www.elsevier.com/locate/jeurceramsoc

Microstructures and mechanical properties of dense particle gels: Microstructural characterisation

Iwan Schenker [a,*], Frank T. Filser [a], Tomaso Aste [b], Ludwig J. Gauckler [a]

[a] *Nonmetallic Materials, Department of Materials, ETH Zurich, Zurich CH-8093, Switzerland*
[b] *Department of Applied Mathematics, RSPhysSE, The Australian National University, 0200 Australia*

Available online 28 January 2008

Abstract

The macroscopic mechanical properties of wet ceramic green bodies and densely packed coagulated colloidal particle gels strongly depend on the local arrangement of the powder particles on length scales of a few particle diameters. Heterogeneous microstructures exhibit up to one order of magnitude higher elastic properties and yield strengths than their homogeneous counterparts. The microstructures of these gels are analysed by the "straight path" method quantifying quasi-linear arrangements of particles. They show similar characteristics than force chains bearing the mechanical load in granular material. Applying this concept to gels revealed that heterogeneous colloidal microstructures show a significantly higher straight path density and exhibit longer straight paths than their homogeneous counterparts.

Keywords: Suspensions; Mechanical properties; Structure and microstructure; Granular matter

1. Introduction

Mechanical properties of coagulated colloids are important in many technical areas. Sediments,[1] ceramic pastes and suspensions,[2] pharmaceutical formulations such as crèmes and emulsions[3] and some food[4] are examples for which it is desirable to control the mechanical properties.

Recently, an internal gelation method (DCC: Direct Coagulation Casting)[5,6] was developed to process electrostatically stabilized suspensions to ceramic green bodies. Thereby it was found that this method permits to control the microstructures of wet ceramic green bodies for solids contents ranging from 20 to 60 vol%. The method allows for an in situ, i.e. undisturbed, destabilization of the colloidal suspension by either changing the pH of the solution (ΔpH-method) resulting in a "homogeneous" microstructure or by increasing the ionic strength (ΔI-method) leading to a "heterogeneous" microstructure.[7]

Fig. 1 shows cryo-SEM pictures of both microstructures. The particles in the ΔpH-coagulated wet green body present a highly homogeneous microstructure whereas in the ΔI-system inhomogeneities on the length scale of a few particle diameters are observed.

This qualitative observation was quantified by the three-dimensional pair-correlation function calculated from stereo cryo-SEM images[7] and by in situ performed diffusing wave spectroscopy (DWS) experiments during destabilization.[8] The structural differences correspond to differences in the heterogeneity: the first peak of the pair-correlation function at $r/d = 1$ (r being the distance between the particles and d the particle diameter) is higher for the ΔI-system indicating locally denser regions with higher average coordination number. Also, local maxima are present in the pair-correlation function for the ΔI-system at $r/d \cong 1.4$ and $\cong 1.6$ corresponding to characteristic peaks in hexagonally packed particle arrangements. During ΔI-destabilization particle rearrangements lead to larger pores and thus to less homogeneous microstructures,[8] whereas during the ΔpH-destabilization the initially stabilized, liquid-like microstructure, is "frozen", which results in a more homogeneous microstructure.

Rheological and uniaxial compression experiments on wet destabilized green bodies obtained by DCC[9,10] showed that colloids with heterogeneous microstructures have significantly higher elastic modulii and yield strengths than their homogeneous counterparts. Measuring the dynamics of the colloids

* Corresponding author. Tel.: +41 44 632 6061; fax: +41 44 632 1132.
E-mail address: iwan.schenker@mat.ethz.ch (I. Schenker).

0955-2219/$ – see front matter © 2007 Elsevier Ltd. All rights reserved.
doi:10.1016/j.jeurceramsoc.2007.12.007

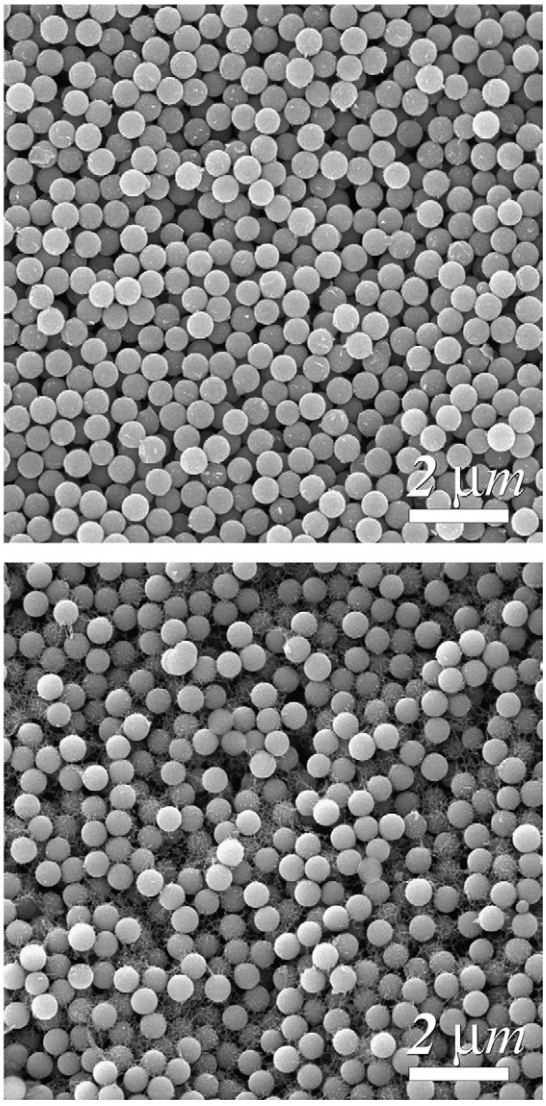

Fig. 1. Microstructure of coagulated silica suspensions at a solids loading of 40 vol% formed by the ΔpH- (a) and the ΔI-method (b) using the DCC process (particle diameter 525 nm). Micrographs obtained by cryo-SEM.[7]

during destabilization by DWS confirmed these findings quantitatively using a model for the storage modulus proposed by Krall and Weitz.[8,11]

Alkali-swellable polymers (ASP) were also used in order to introduce heterogeneities during the ΔpH-destabilization. Small amounts of 80 nm ASP particles were admixed to the powders under acidic conditions. These particles swell upon changing pH during the internal gelling reaction of the DCC process and enfold to 800 nm size producing less homogeneous microstructures. Those samples with swollen polymer particles showed much higher mechanical properties in comparison to samples without swellable polymers and hence more homogenous microstructures.[12] These samples present the same high mechanical properties as samples with heterogeneous microstructures produced by the ΔI-method.[12]

Examples of the rheologically measured elastic properties of mono-dispersed silica particle suspensions (particle diameter 200 nm) for different solids loadings destabilized by the ΔpH- and the ΔI-method, respectively, are shown in Fig. 2. Almost one order of magnitude higher elastic plateau storage modulii are measured for heterogeneous microstructures than for those with homogenous microstructures.[10]

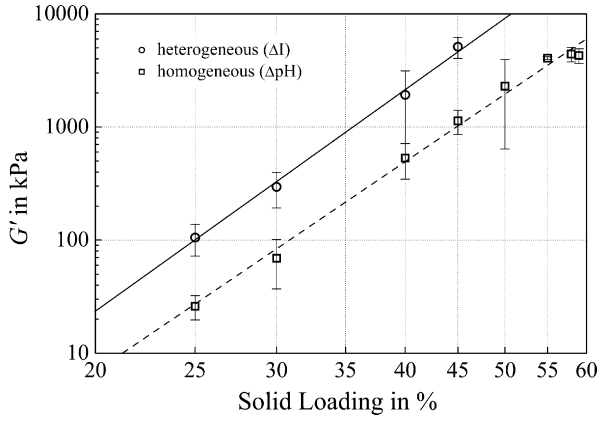

Fig. 2. Elastic plateau storage modulus G' of silica particle suspensions (particle diameter 200 nm) in dependence of the solids loading formed by the ΔpH- and the ΔI-method of the DCC process.[10]

In summary, strong evidence is given that the differences in macroscopic mechanical properties of coagulated particle suspensions are controlled by the differences in microstructure. An open question is now how these microstructural differences on particle length scales can have such a dramatic influence on the mechanical properties. Therefore, a concise quantitative analysis of microstructures of colloidal particle systems is needed.

In preceding works, various characterization methods, such as the radial pair-correlation function,[13] the bond angle distribution function,[13] the triangle distribution function[13] and the Minkowski functionals in conjunction with the parallel-body technique,[14] were applied to sets of microstructures generated by Brownian dynamics (BD) simulations.[15] These simulations were used to study the coagulation dynamics and the evolving microstructures in dense colloidal suspensions and the resulting microstructures agree well with experiments.[16]

While the pair-correlation function permits to quantify the amount of structural rearrangement during the coagulation,[13] the analysis using the Minkowski functionals in conjunction with the parallel-body technique supplies additional information on the structure's morphology resolving microstructural differences on a length scale limited by the largest pore size.[14] The bond angle distribution function and the triangle distribution functions are useful means to examine the local building blocks of the particle network.[13] Particular features, as for example, peaks in the respective distribution function have successfully been correlated to the structure's heterogeneity and porosity. The same conclusion is valid for the Minkowski functionals.[14]

All these four methods are good means to compare structures in terms of their heterogeneity. However, these structural descriptions do not unambiguously help to understand why more heterogeneous colloidal structures possess stronger mechanical properties as they do not adequately capture the microstructural characteristics that are responsible for the mechanical properties of these particle systems.

It is well known from granular matter physics that particulate systems under mechanical stress carry load via *chains of contacting particles*, termed *force chains*, as observed in experiments on granular materials[17] and in simulations.[18] Granular materials, as for example sand piles, that contain large amounts of particles arranged in *chains of contacting particles* are expected to possess higher mechanical properties than those in which the particles have to rearrange upon applied external load in order to form such chains. Hence it is plausible that these chains of contacting particles control the mechanical properties.

The aim of this paper is to adequately analyse the microstructure of dense colloids, to capture their degree of heterogeneity and to link microstructural differences to differences in macroscopic mechanical properties upon applied mechanical stress.

Thereby we focus on the identification of *densely packed regions* and *chains of contacting particles* in these particle networks that may correlate differences in mechanical properties with differences in microstructures. Our approach is to analyse the distribution of densely packed regions in each microstructure using the *common neighbour distribution* and the *dihedral angle distribution function.* Additionally, we introduce a new method that we call the "*straight path"* method, characterizing the *quasi-linear arrangement of particle chains*. The evaluation of these characterization methods is performed with regard to their ability to distinguish quantitatively between homogeneous and heterogeneous microstructures obtained from BD simulations[15] mimicking well those found in experiments.[16]

2. Materials and methods

2.1. Structure generation

The homogeneous and the heterogeneous microstructures are fully coagulated colloidal suspensions obtained from Brownian dynamics simulations.[15] The DLVO theory[19] was used to describe the particle–particle interaction, where pair-wise particle potential interactions are assumed given by the sum of the van der Waals attraction V^{vdw} (Eq. (1)) and the electrostatic double layer repulsion V^{el} (Eq. (2)). Thus, $V^{\mathrm{dlvo}} = V^{\mathrm{vdw}} + V^{\mathrm{el}}$ with,

$$V^{\mathrm{vdw}}(r) = -\frac{A_{\mathrm{H}}}{12}\left[\frac{d^2}{r^2-d^2} + \frac{d^2}{r^2} + 2\ln\left(\frac{r^2-d^2}{r^2}\right)\right] \quad (1)$$

and

$$V^{\mathrm{el}}(r) = \pi\varepsilon_{\mathrm{r}}\varepsilon_0\left[\frac{4k_{\mathrm{B}}T}{ze}\tanh\left(\frac{ze}{4k_{\mathrm{B}}T}\Psi_0\right)\right]^2 d\exp(-\kappa\{r-d\}), \quad (2)$$

respectively. The DLVO parameters are summarized in Table 1 and the potential curves for various values of the surface potential Ψ_0 are shown in Fig. 3.

For $\Psi_0 = 0$ mV, the electrostatic double layer repulsion is zero and the inter-particle potential is only given by the attractive van der Waals potential. For $\Psi_0 \geq 12$ mV a secondary minimum appears and ΔE denotes the energy barrier between the local maximum and the secondary minimum. For $\Psi_0 = 15$ mV, a repulsive barrier of $\Delta E \cong 5.65\, k_{\mathrm{B}}T$ exists and the secondary minimum is found at $r = 1.08\, d$. The model further contains the frictional Stokes' drag force and a random Brownian force caused by the suspending liquid.

Table 1
Potential parameters for the coagulating suspensions

Parameter	Symbol	Value
Hamaker constant of Al_2O_3 in water	A_{H}	4.76×10^{-20} J
Particle diameter	d	5×10^{-7} m
Relative dielectric constant of water	ε_{r}	81
Absolute temperature	T	20 °C
Valency of ions	z	1
Inverse Debye screening length	κ	10^8 m^{-1}

We analyse microstructures generated using $\Psi_0 = 0$ mV, which correspond to the ΔpH-destabilization method and $\Psi_0 = 15$ mV, corresponding to the ΔI-destabilization method. In the following we label the ΔpH-microstructures as homogeneous and the ΔI-microstructures as heterogeneous. All structures have the same solids loading of 40 vol% and contain 8000 spherical particles forming one percolating cluster. The particles have a diameter of 500 nm.

2.2. Structure characterization methods

2.2.1. Common neighbour and dihedral angle distribution function

The common neighbour analysis[20] considers pairs of particles, referred to as configurations, and determines the number of particles that are in contact with both particles of the configuration. In two dimensions, configurations can have at most two common neighbours. In three dimensions, configurations can have up to five common neighbours. The number of configurations with n common neighbours is denoted CN_n with $n = 1, \ldots, 5$. In this study, absolute numbers of configurations are compared as the microstructures analysed have identical solids loading, the same number of particles and equal particle diameters.

The common neighbour distribution describes the short range arrangement of particles. In particular, CN_0 is the number of

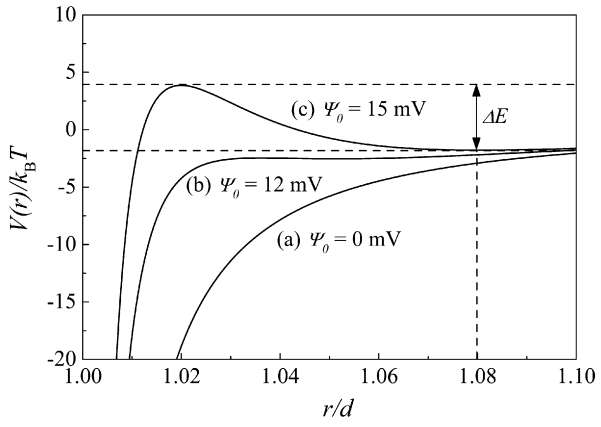

Fig. 3. DLVO-interaction for different surface potentials: (a) pure van der Waals attraction (ΔpH-destabilization), (b) $\Delta E/k_{\mathrm{B}}T = 0$ and (c) $\Delta E/k_{\mathrm{B}}T = 5.65$ (ΔI-destabilization).

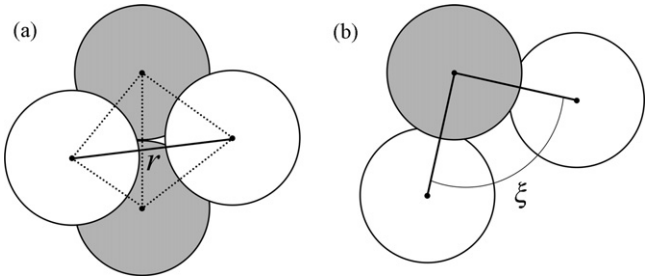

Fig. 4. Configuration (grey particles) with two common neighbours separated by a distance r and having a dihedral angle ξ. Perspective view (a) and top view (b).

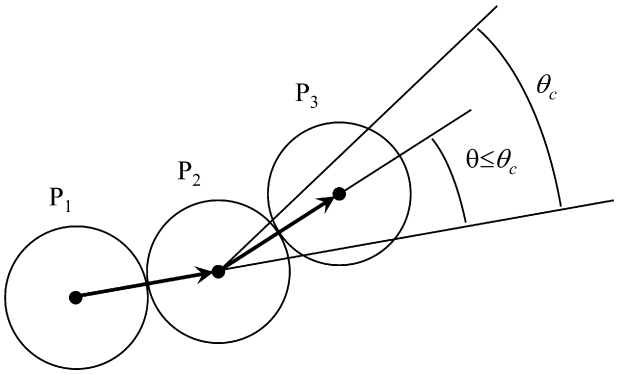

Fig. 5. Chain of three particles forming a straight path.

pairs of contacting particles with no common neighbour. CN_1 counts the number of configurations with exactly one neighbour common to both particles, forming equilateral triangles. For $n=2$ the four particles of the configuration form a regular tetrahedron if the two common neighbours are in contact, and a generalized tetrahedron, having one longer edge, otherwise.

Configurations with two or more common neighbours (CN_2, …, CN_5) can be further characterized by the dihedral angle distribution that analyses the arrangement of the neighbouring particles around the two particles of the configuration, which form regular triangles with each of their common neighbours. For $n \geq 2$ there are at least two common neighbours. In this case, the dihedral angle ξ is defined as the angle between two planes spanned by triangles belonging to the same configuration as shown in Fig. 4. ξ is measured between one triangle and the triangles formed with each other common neighbour of the original couple of particles. Chemistry uses this method to characterize molecular structures.[21] In the field of granular matter the dihedral angle distribution has been used to study the structural organization and correlations in very large packings of mono-dispersed spherical particles.[22,23]

For two common neighbours in contact with each other, the four particles form a regular tetrahedron and the dihedral angle is 70.5°. This angle constitutes the lower limit of the dihedral angle distribution. The upper limit is 180° when the four particles are in a plane and form a square.

Formally, the dihedral angle ξ between two common neighbours of a configuration having a separation distance r between each other is defined by $\xi = 2 \times \arcsin(r/\sqrt{3}d)$. The dihedral angle distribution[23] is given by $p(\xi + \delta\xi/2) = \delta N_\xi(\xi, \xi + \delta\xi)$ where $\delta N_\xi(\xi, \xi + \delta\xi)$ is the number of generalized (open) tetrahedra with a dihedral angle between ξ and $\xi + \delta\xi$.

2.2.2. Straight path method

A straight path is a quasi-linear chain of contacting particles. The shortest chain consists of three particles. In order for three particles to form a straight path they have to fulfil the following condition: the angle θ between the vector connecting the first two particles (P_1, P_2) and the vector connecting the second two particles (P_2, P_3) must be smaller than a chosen threshold angle θ_c. This is exemplified in Fig. 5.

Analogously, a straight path of length l is one of length $l-1$ that has another particle attached to one end and whose connection vector fulfils the condition to stay in a direction within a cone of angle θ_c from the vector connecting the previous two particles. The distribution of straight path lengths is obtained by determining the number of straight paths SP_l of length l for $l=1$ to l_{max}, with l_{max} the longest path under consideration. Absolute numbers are calculated and compared in the distribution of SP_l.

The angle θ_c determines the quasi-linearity and specifies the maximally allowed deflection from an absolute linear arrangement of the particles. The dependence of the straight path statistic on the angle θ_c is presented as part of the results section and is used in order to choose a suitable angle θ_c.

The distribution of straight paths for the homogeneous and heterogeneous microstructures is compared. The average path length $SP_{mean} = \sum_{l\geq 3} l\, SP_l / \sum_{l\geq 3} SP_l$ and the number of paths longer than a chosen length l_0 is determined. The latter is defined by $SP_{l\geq l_O} = \sum_{l\geq l_O} SP_l$ ($l_0 = 4$ and 5) and permits to quantify differences in the number of straight paths with longer lengths, neglecting paths shorter than l_0 particles.

3. Results and discussion

3.1. Common neighbour analysis

The number of particle configurations CN_n is higher for the heterogeneous than for the homogeneous microstructure for $n=0, \ldots, 3$ (Fig. 6). This can easily be understood as the mean coordination number of a particle in the heterogeneous microstructure is with 5.2 roughly 10% larger than in the homogeneous microstructures with 4.7. When normalized by the mean coordination number, the distributions collapse, indicating that the relative distribution of common neighbour configurations is identical for both microstructures. Therefore we conclude that the common neighbour distribution does not capture in a suitable way the structural differences between these microstructures.

3.2. Dihedral angle distribution

The dihedral angle distributions of both microstructures show a characteristic peak at 70.5° (Fig. 7) corresponding to configurations that form regular tetrahedra with two common neighbours. The peak height is the same for both microstructures. The heterogeneous microstructure has a peak at 77°, which is missing for the homogeneous one. This angle corresponds to a separa-

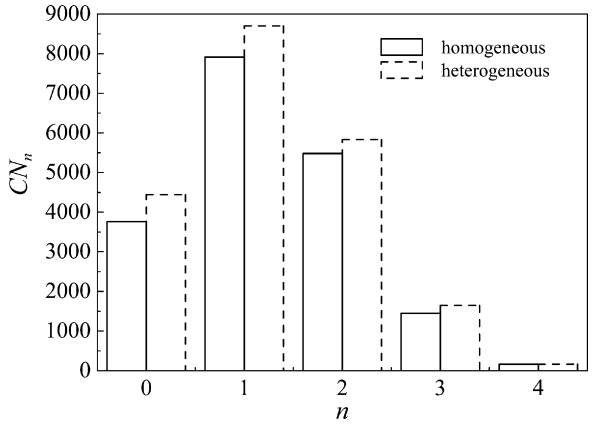

Fig. 6. Common neighbour distribution for the homogeneous and heterogeneous microstructures: number of configurations CN_n in dependence of the number of common neighbours n.

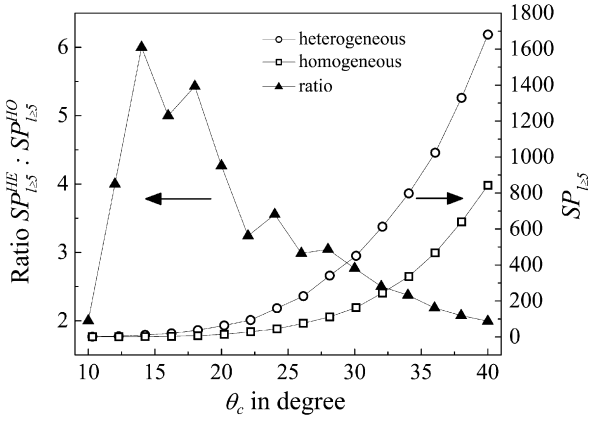

Fig. 8. Number of straight paths for both microstructures longer or equal to five ($SP^{HE}_{l\geq5}$ and $SP^{HO}_{l\geq5}$, open symbols) and their ratio ($SP^{HE}_{l\geq5} : SP^{HO}_{l\geq5}$, triangles) as a function of the threshold angle θ_c.

tion distance between the common neighbours of $1.08\,d$ which is the distance between particles trapped in the secondary minimum (Fig. 3). At $\xi = 109.5^\circ$ the homogeneous microstructure has a peak that corresponds to a common neighbour separation of $1.41\,d \cong \sqrt{2}\,d$, which is absent in the case of the heterogeneous microstructure. This separation distance corresponds to two configurations forming a square and sharing two common neighbours. An additional characteristic peak is found at 141° having roughly the same height for both microstructures and corresponding to two juxtaposed tetrahedra. The peak at 148° is solely present for the heterogeneous microstructure and corresponds to one regular tetrahedron juxtaposed to one with a distance of $1.08\,d$ between the common neighbours.

In conclusion, even if there are sizable differences between homogeneous and heterogeneous structures, the absolute number of regular tetrahedra is virtually equal for both microstructures and the analysis does not reveal any structural difference that could explain the better mechanical properties of the heterogeneous microstructures. We therefore conclude that the common neighbour and the dihedral angle distributions are not suited to link the microstructural differences to the different mechanical properties.

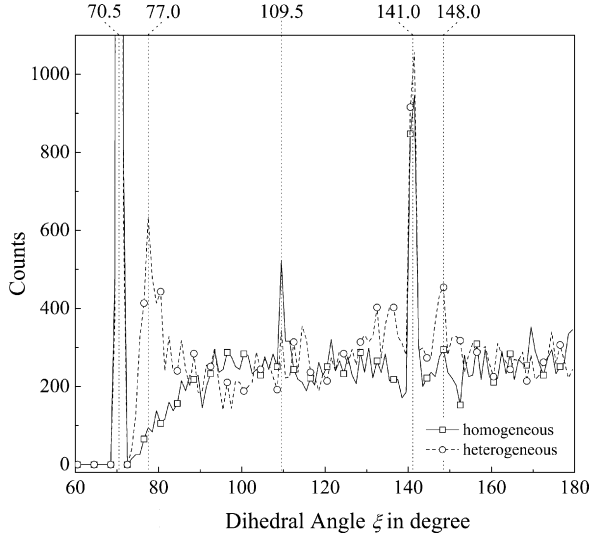

Fig. 7. Dihedral angle distribution for the homogeneous and heterogeneous microstructures. For clarity purposes, only every fourth data point is indicated by a symbol.

3.3. Straight path analysis

The straight path analysis depends on the threshold angle θ_c, hence, a suitable value θ_c has to be determined. For small angles θ_c only a small number of straight paths are expected because only a few particle chains satisfy the criterion to be a straight path. For large angles θ_c many straight paths are found but the physical meaning of a straight path is lost as the path becomes less "straight" and thus loses its load bearing capacity. Also for increasing θ_c the ratio of the number of paths with equal lengths between the heterogeneous and the homogeneous microstructure decreases. Fig. 8 shows the number of straight path longer or equal to five particles for the homogeneous ($SP^{HO}_{l\geq5}$) and for the heterogeneous microstructure ($SP^{HE}_{l\geq5}$) as well as their ratio ($SP^{HE}_{l\geq5} : SP^{HO}_{l\geq5}$) in dependence of the cone angle θ_c ranging from 10° to 40°. The lines serve as guide to the eye.

For θ_c between 14° and 18° the ratio $SP^{HE}_{l\geq5} : SP^{HO}_{l\geq5}$ shows a maximum. However, below 22° the number of straight paths is quite small ($SP_{l\geq5} < 100$) for both microstructures. Towards larger angles the absolute number of straight paths is increasing while the ratio $SP^{HE}_{l\geq5} : SP^{HO}_{l\geq5}$ is decreasing. The angle $\theta_c = 30^\circ$ was chosen as this angle gives reasonable values for both the ratio ($SP^{HE}_{l\geq5} : SP^{HO}_{l\geq5} \cong 3$) and absolute number of paths ($SP^{HE}_{l\geq5} = 451$ and $SP^{HO}_{l\geq5} = 163$).

For both microstructures the distribution of straight paths shows an exponential decrease with straight path length l_{SP} (Fig. 9). Both microstructures have approximately the same number of straight paths of length three. Towards longer path lengths the microstructures present a diverging behaviour: the heterogeneous microstructure has more paths of longer length than the homogeneous microstructure. The distributions were fitted by an exponential law using $SP_l \propto \exp(-\beta l_{SP})$. A remarkably good fit of the data is obtained for both microstructures indicated by the values close to one for the coefficients of deter-

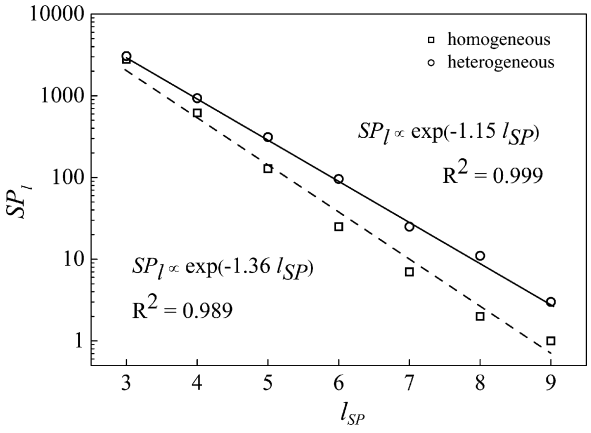

Fig. 9. Number of straight paths SP_l in dependence of the straight path length l_{SP} for the homogeneous and heterogeneous microstructures (squares and circles, respectively) and exponential fits (dashed and solid line, respectively).

mination R^2. The higher exponent β found for the homogeneous microstructure demonstrates the more rapid decrease of the number of straight paths towards longer path lengths than in the case of the heterogeneous microstructure.

The values for the average path lengths (SP_{mean}) and the numbers of paths longer or equal to four ($SP_{l\geq4}$) and five ($SP_{l\geq5}$) are summarized in Table 2.

The average path length for the heterogeneous microstructure is only 5% longer than for the homogeneous microstructure because $SP_{l=3}$ dominates the statistics and is almost identical for both structures. On the other hand, in the heterogeneous microstructure longer chains $SP_{l\geq4}$ and $SP_{l\geq5}$ are found 1.8 and 2.8 times more often, respectively, than in the homogeneous one.

To conclude, the number of straight paths in our homogeneous and heterogeneous microstructures follows an exponential distribution and the higher exponent β is found for the homogeneous microstructure. The heterogeneous microstructure contains significantly more straight paths of longer lengths than the homogeneous one: in absolute numbers we observe twice as many paths with a length ≥ 4 and three times as many having a length ≥ 5. These are very significant differences between the two microstructures.

Our results suggest that the differences in the straight path distributions are characteristic for the better mechanical properties of the heterogeneous microstructures. Indeed, in granular materials load is transmitted via force chains that are quasi-linear substructures of the particle network. This has been experimentally verified using photo-elasticity techniques[17] and computationally modelled using the discrete element method (DEM).[18] Also, the computational study of the force chain network in 2D granular assemblies of polydispersed particles subjected to indentation by a rigid flat punch has shown that the force chain length follows an exponential distribution.[24]

Table 2
Average path length SP_{mean} and number of paths longer or equal to four ($SP_{l\geq4}$) and five ($SP_{l\geq5}$) for both microstructures

Microstructure	Homogeneous	Heterogeneous
SP_{mean}	3.28	3.45
$SP_{l\geq4}$	779	1385
$SP_{l\geq5}$	163	451

4. Conclusions

Different chemical pathways during the internal destabilization of colloidal suspensions lead to wet ceramic green bodies with drastically different mechanical properties. The microstructures of these destabilized colloids reveal differences in the homogeneity of the particle arrangements on a length scale in the order of a few particle diameters. We applied different microstructural characterization methods, i.e. common neighbour distribution, dihedral angle distribution and straight path method, to analyse homogeneous and heterogeneous microstructures generated by Brownian dynamics simulations, which were shown to agree well with the experimentally determined microstructures of such coagulated colloidal particle systems.

Towards our goal, to establish a correlation between the microstructural differences and the differences in macroscopic mechanical properties, we found that the common neighbour and the dihedral angle distributions do not discriminate enough the differences between the homogeneous and heterogeneous microstructures and can therefore hardly account for the large differences in mechanical properties. The newly introduced "straight path" method reveals significantly more straight paths of longer lengths for the heterogeneous than for the homogenous microstructure: two times more straight paths of length ≥ 4 particles and three times more of length ≥ 5 particles are found in the heterogeneous microstructure. These differences in straight path number and length seem suitable to characterize and to differentiate between these structures and we consider these differences sufficiently large to account for the differences in mechanical properties. The straight paths may capture best the characteristic microstructural features which are relevant for the mechanical properties. We found that the number of straight paths follows an exponential distribution just like the distribution of the force chain length in mechanically loaded granular material.[24] Additionally, the quasi-linear structure of the straight paths seems to correspond to the geometrical shape of force chains[17,18] that are well known to determine the load bearing capacity of granular matter. These findings are encouraging for an attempt to establish a correlation between defined microstructural features and the differences in mechanical properties of destabilized colloids.

Further quantitative structural analyses and computational modelling using the discrete element method are in progress to study the force chains in ceramic green bodies and to correlate them with the straight paths of their microstructures.

Acknowledgment

The authors would like to express their gratitude to Markus Hütter for providing the colloidal microstructure data from the Brownian dynamics simulations.

References

1. Yun, T. S., Santamarina, J. C. and Ruppel, C., Mechanical properties of sand, silt, and clay containing tetrahydrofuran hydrate. *J. Geophys. Res.*, 2007, **112**, B04106.
2. Feng, J.-H. and Dogan, F., Aqueous processing and mechanical properties of PLZT green tapes. *Mater. Sci. Eng. A*, 2000, **283**, 56–64.
3. Adeyeye, M. C., Jain, A. C., Ghorab, M. K. M. and Reilly Jr., W. J., Viscoelastic evaluation of topical creams containing microcrystalline cellulose/sodium carboxymethyl cellulose as stabilizer. *AAPS Pharm. Sci. Technol.*, 2002, **3**(2) (article 8).
4. Marti, I., Höfler, O., Fischer, P. and Windhab, E. J., Rheology of concentrated suspensions containing mixtures of spheres and fibres. *Rheol. Acta*, 2005, **44**, 502–512.
5. Gauckler, L. J., Graule, Th. and Baader, F., Ceramic forming using enzyme catalyzed reactions. *Mater. Chem. Phys.*, 1999, **61**, 78–102.
6. Tervoort, E., Tervoort, T. A. and Gauckler, L. J., Chemical aspects of direct coagulation casting of alumina suspensions. *J. Am. Ceram. Soc.*, 2004, **87**(8), 1530–1535.
7. Wyss, H. M., Tervoort, E., Meier, L. P., Müller, M. and Gauckler, L. J., Relation between microstructure and mechanical behavior of concentrated silica gels. *J. Colloid Interface Sci.*, 2004, **273**, 455–462.
8. Wyss, H. M., Tervoort, E., Meier, L. P., Müller, M. and Gauckler, L. J., Diffusion-wave spectroscopy of concentrated alumina suspensions during gelation. *J. Colloid Interface Sci.*, 2001, **240**, 89–97.
9. Balzer, B., Hruschka, M. K. M. and Gauckler, L. J., Coagulation kinetics and mechanical behavior of wet alumina green bodies produces via DCC. *J. Colloid Interface Sci.*, 1999, **216**, 379–386.
10. Wyss, H. M., Deliormanli, A. M., Tervoort, E. and Gauckler, L. J., Influence of microstructure on the rheological behavior of dense particle gels. *AIChE J.*, 2005, **51**(1), 134–141.
11. Krall, A. H. and Weitz, D. A., Internal dynamics and elasticity of fractal colloidal gels. *Phys. Rev. Lett.*, 1998, **80**(4), 778–781.
12. Hesselbarth, D., Quellfähige Polymerbinder in Aluminiumoxid-Suspensionen, Ph.D. Thesis No. 13404, ETH Zurich, Switzerland, 2000. http://e-collection.ethbib.ethz.ch/show?type=diss&nr=13404.
13. Hütter, M., Local structure evolution in particle network formation studied by brownian dynamics simulation. *J. Colloid Interface Sci.*, 2000, **231**, 150–337.
14. Hütter, M., Heterogeneity of colloidal particle networks analysed by means of Minkowski functionals. *Phys. Rev. E*, 2003, **68**, 031404.
15. Hütter, M., Brownian dynamics simulation of stable and of coagulating colloids in aqueous suspension, Ph.D. Thesis No. 13107, ETH Zurich, Switzerland, 1999. http://e-collection.ethbib.ethz.ch/show?type=diss&nr=13107.
16. Wyss, H. M., Hütter, M., Müller, M., Meier, L. P. and Gauckler, L. J., Quantification of microstructures in stable and gelated suspensions from cryo-SEM. *J. Colloid Interface Sci.*, 2002, **248**, 340–346.
17. Drescher, A. and de Josselin de Jong, G., Photoelastic verification of a mechanical model for the flow of a granular material. *J. Mech. Phys. Solids*, 1972, **20**, 337–351.
18. Cundall, P. A. and Starck, D. L., A discrete numerical model for granular assemblies. *Géotechnique*, 1979, **29**, 47–65.
19. Russel, W. B., Saville, D. A. and Schowalter, W. R., *Colloidal Dispersions*. Cambridge University Press, 1989.
20. Clarke, A. S. and Jónsson, H., Structural changes accompanying densification of random hard-sphere packings. *Phys. Rev. E*, 1993, **47**(6), 3975–3984.
21. Wielopolski, P. A. and Smith, E. R., Dihedral angle distribution in liquid *n*-butane: molecular dynamics simulations. *J. Chem. Phys.*, 1986, **84**(12), 6940–6942.
22. Aste, T., Variations around disordered closed packing. *J. Phys.: Condens. Matter*, 2005, **17**, S2361–S2390.
23. Aste, T., Volume fluctuations and geometrical constraints in granular packs. *Phys. Rev. Lett.*, 2006, **96**, 018002.
24. Peters, J. F., Muthuswamy, M., Wibowo, J. and Tordesillas, A., Characterization of force chains in granular material. *Phys. Rev. E*, 2005, **72**, 041307.